

# Laser Doppler anemometer signal processing for blood flow velocity measurements

M.A. Borozdova, I.V. Fedosov, V.V. Tuchin

**Abstract.** A new method for analysing the signal in a laser Doppler anemometer based on the differential scheme is proposed, which provides the flow velocity measurement in strongly scattering liquids, particularly, blood. A laser Doppler anemometer intended for measuring the absolute blood flow velocity in animal and human near-surface arterioles and venules is developed. The laser Doppler anemometer signal structure is experimentally studied for measuring the flow velocity in optically inhomogeneous media, such as blood and suspensions of scattering particles. The results of measuring the whole and diluted blood flow velocity in channels with a rectangular cross section are presented.

**Keywords:** laser Doppler anemometer, blood, microcirculation, light scattering, digital signal processing.

## 1. Introduction

Laser Doppler anemometers (LDAs) [1–5] and Doppler optical coherence tomographs (DOCTs) [6–9] are widely used in medical diagnostics and physiology studies. In contrast to most optical methods of microcirculation study, such as intravital microscopy [10, 11], optical coherence [12] and fluorescence [13] angiography, scanning laser Doppler flowmetry [14] and laser speckle contrast analysis [15, 16], targeted at imaging the vascular network and estimating the relative change of the circulating blood volume, LDAs and DOCTs allow the measurement of the blood flow velocity and precise evaluation of the volume flow rate in individual arterioles and venules. The availability of such measurements is of critical importance for early diagnostics of the visual nerve atrophy in the cases of glaucoma and diabetic retinopathy [1–3, 9]. It is also necessary for understanding the fundamental mechanisms of local blood flow in organs and tissues, e.g., in the cases of cerebral stroke [16] or myocardium ischemia [17].

The LDA and DOCT operating principle is based on measuring the Doppler frequency shift (DFS) of optical radiation singly scattered by moving cells. The DFS value is proportional to the projection of the velocity vector on the direction of the light scattering vector, defined as the difference of

incident and scattered wave vectors [4, 18, 19]. The absolute value of the flow velocity can be determined if the angle between the velocity vector and the scattering vector is known. Since this angle cannot be directly found in *in vivo* measurements, the absolute value and the direction of the blood flow velocity vector are determined by measuring the DFS of radiation scattered simultaneously in two or three different directions, like, e.g., in the ophthalmologic LDAs aimed at the diagnostics of microcirculation disturbances in eye retina vessels [1–4]. The application of a similar approach in DOCTs is associated with great technical difficulties [20], that is why for DOCTs it was proposed to determine the spatial position of a blood vessel by scanning two closely spaced cross sections of one vessel [21], or excluding the uncertainty in the evaluation of the blood volume flow rate by integrating the flow velocity over the vessel cross section [22]. The implementation of DOCTs for *in vivo* measurements of all three components of the velocity vector by recording radiation scattered in several directions, became possible only recently due to the development of Fourier-DOCT methods, providing the necessary operation speed [8, 9].

LDAs and DOCTs are mainly used for studying the vessels located at a small depth parallel to the surface of a strongly scattering tissue. The tissue is illuminated perpendicular to its surface and the backscattered radiation is detected. In this case, the scattering vector is practically perpendicular to the axis of the studied blood vessel; the DFS strongly depends on the angle between the flow velocity vector and the scattering vector and turns into zero when this angle equals  $90^\circ$ . On the other hand, if the velocity vector makes a small angle with the scattering vector, then the dependence of DFS on the angle can be neglected. For example, when the angle varies from  $-10^\circ$  to  $+10^\circ$ , the error of the velocity measurement does not exceed 1.5%.

In experimental aero- and hydrodynamics LDAs based on the differential scheme (differential LDAs) are widely used, in which the moving particle is simultaneously illuminated with two laser beams crossing at a small angle [18, 19]. As a result, radiation scattered by the particle in any direction appears to be modulated with the frequency, proportional to the projection of the velocity vector on the so called LDA sensitivity vector. The sensitivity vector, defined as the difference of wave vectors of the laser beams, is oriented perpendicular to the LDA optical axis. The modulation frequency is independent of the light scattering direction and the refractive index of the medium [19], surrounding the moving particle, which is important in the measurements of the blood flow velocity, for which the refractive index in the particular vessel is, as a rule, unknown. In spite of the obvious advantage over the existing methods, the differential LDA still has not found

M.A. Borozdova, I.V. Fedosov N.G. Chernyshevsky Saratov State University, ul. Astrakhanskaya 83, 410012 Saratov, Russia; e-mail: mariabor@mail.ru;

V.V. Tuchin N.G. Chernyshevsky Saratov State University, ul. Astrakhanskaya 83, 410012 Saratov, Russia; Institute of Problems of Precision Mechanics and Control, Russian Academy of Sciences, ul. Rabochaya 24, 410028 Saratov, Russia; e-mail: tuchinvv@mail.ru

Received 29 August 2014; revision received 28 October 2014

Kvantovaya Elektronika 45 (3) 275–282 (2015)

Translated by V.L. Derbov

application in the blood microcirculation studies, except a limited number of papers in the field of laser Doppler microscopy [23, 24].

The limited application of the differential LDA to the measurement of the flow velocity in blood and other strongly scattering liquids is mainly caused by the difficulty of Doppler frequency shift measurement against the background of fluctuating intensity of light scattered by the particles that move beyond the probe volume. At present the main way of solving this problem is to introduce a shift between the laser beam frequencies in the differential LDA using optical modulators [23] or tunable optical delay lines [24].

In this paper we propose a new method of extracting the useful components of the laser radiation power fluctuation spectrum, caused by the motion of scattering particles within the probe volume and carrying the information about the flow velocity. The proposed method is based on the intensity modulation of the laser beams and does not require any devices for preliminary introduction of a frequency shift between them. The experimental testing of the proposed method, as well as the detailed study of the LDA signal structure in the process of measuring the flow velocity in strongly scattering liquids were carried out using the differential LDA, developed by the authors. The results of measuring the flow velocity in a scattering liquid and blood in channels with a rectangular-shaped cross section are presented.

## 2. Materials and methods

### 2.1. Laser Doppler anemometer

A schematic diagram of the developed LDA is presented in Fig. 1. An ML-09 semiconductor laser unit (Skat-R, Russia) with the radiation wavelength 650 nm and the power 15 mW was used as a light source. By means of the rhomb prism the

laser radiation beam was split into two parallel beams that were focused in the studied region of the liquid flow by means of objective 1 with the focal length 100 mm and the aperture 30 mm. A polarisation filter and a quarter-wave plate, which protects the cavity of the semiconductor laser from the retrieval of radiation specularly reflected by the studied object towards the LDA objective, were installed between the laser and the rhomb prism.

The LDA probe volume is formed by the crossing of mutually coherent beams of laser radiation. In the probe volume a system of interference fringes transverse with respect to the flow direction is produced. Radiation scattered by the particles suspended in the liquid passes through objective 1 in the backward direction and is reflected by the mirror towards another objective 2. Objective 2 identical to objective 1 produces an image of the probe volume in the plane of the circular field stop with the diameter 50  $\mu\text{m}$ , placed in front of the FD-256 photodiode. The photodetector signal was amplified and then recorded by means of the personal computer sound card.

The LDA optical system is mounted on a horizontal base in such a way, that the laser beams forming the probe volume are located in a horizontal plane  $xz$ , and the  $y$  axis is directed straight up.

### 2.2. Probe volume assessment and LDA alignment

The used multifrequency semiconductor laser generates a single transverse mode. The built-in collimator of the laser unit forms the laser beam with the divergence 6 mrad. The laser unit beam cross section is nearly rectangular-shaped with rounded corners and the dimensions  $2 \times 5$  mm. This beam is divided into two parallel beams with the cross sections  $2 \times 2$  mm by means of the rhomb prism. The beams are focused in the front focal plane of objective 1 (Fig. 1) crossing in the waist regions

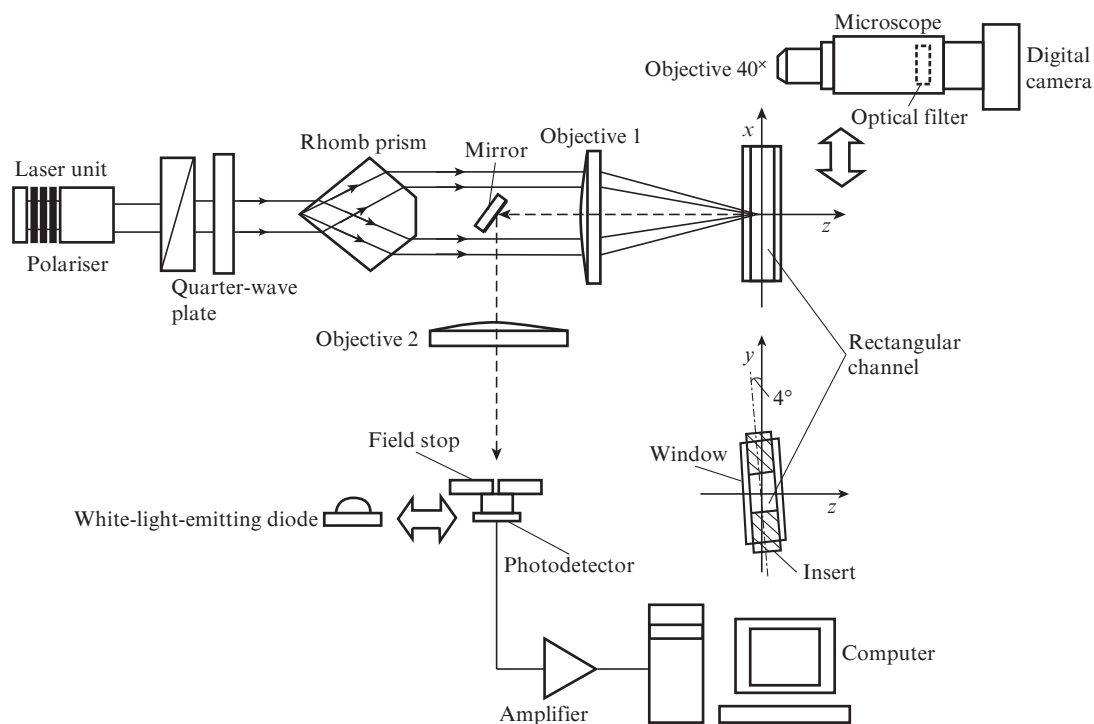


Figure 1. Schematic diagram of the experimental setup.

at the angle  $14^\circ$ . The precision of the beam coincidence is determined by the alignment of the LDA optical system and the accuracy of the prism fabrication.

The LDA alignment and assessment of the actual shape and dimension of the probe volume was implemented using the microscope, consisting of a 137-mm-long drawtube, an objective ( $40\times, 0.65$ ), and a DSB-C320 digital camera (D-link, Taiwan). A blue optical filter was mounted inside the microscope drawtube to limit the laser radiation intensity arriving at the digital camera image sensor. The microscope is installed coaxially with objective 1 of the LDA on the magnetic base interchangeable with the base of the studied object holder. The displacement of the microscope along the LDA optical axis is implemented by means of the micrometre screw device. The scale of the image in the object plane of the microscope was determined using a stage micrometer. The dimensions of the probe volume were determined in air at the level  $e^{-2}$  of the maximal intensity at a fixed exposure time of the digital camera.

The observation of the probe volume has shown that the laser beams almost completely overlap in the region of their smallest cross section. The probe volume in the region of complete overlap of the laser beams has a practically circular cross section with a diameter  $60\ \mu\text{m}$ . The contrast of interference fringes within this cross section is close to 1, and the period of the interference fringes is equal to  $\sim 2.7\ \mu\text{m}$ . The length of the probe volume amounts to  $110\ \mu\text{m}$ .

To perform the alignment of the detector field stop position the photodiode was replaced with a white-light-emitting diode with a power of 3 W. Simultaneously, the observation of the probe volume and the circular field stop with a diameter  $50\ \mu\text{m}$  was carried out using the microscope. By means of adjusters the field stop was moved in three dimensions to match its image with the minimal cross section of the probe volume.

### 2.3. LDA signal analysis

The LDA probe volume is formed by two beams of laser radiation with similar frequencies  $\omega_0$  crossing at the angle  $\alpha = 14^\circ$  (Fig. 2). Due to the Doppler effect, radiation of beam 1, scattered by the moving particle towards the detector, acquires the frequency [18, 19]

$$\omega_1 = \omega_0 - (\mathbf{k}_s - \mathbf{k}_{i1})\mathbf{u} = \omega_0 - \mathbf{K}_1\mathbf{u}, \quad (1)$$

where  $\mathbf{k}_{i1}$ ,  $\mathbf{k}_s$  are the wave vectors of the incident and scattered beams; and  $\mathbf{u}$  is the velocity of the scattering particle motion. Similarly, the radiation frequency of beam 2, scattered towards the detector, is

$$\omega_2 = \omega_0 - (\mathbf{k}_s - \mathbf{k}_{i2})\mathbf{u} = \omega_0 - \mathbf{K}_2\mathbf{u}, \quad (2)$$

where  $\mathbf{k}_{i2}$  is the wave vector of beam 2. As a result of the interference of the fields having the frequencies  $\omega_1$  and  $\omega_2$ , the radiation intensity at each point of the detector varies according to the law [18]

$$I_d(t) = I_1 + I_2 + 2\sqrt{I_1 I_2} \cos(\omega_d t + \delta), \quad (3)$$

where  $I_1$ ,  $I_2$  are the intensities of radiation with the frequencies  $\omega_1$  and  $\omega_2$ , respectively; and  $\delta$  is a certain constant phase difference, caused by the geometry of the experiment. The modulation frequency is determined from Eqns (1) and (2) as

$$\omega_d = \omega_1 - \omega_2 = (\mathbf{k}_{i1} - \mathbf{k}_{i2})\mathbf{u} = \mathbf{K}\mathbf{u}, \quad (4)$$

where  $\mathbf{K}$  is the wave vector difference, directed perpendicular to the LDA optical axis. The magnitude of the vector  $\mathbf{K}$  is determined by the relation [18]

$$|\mathbf{K}| = \frac{4\pi}{\lambda} \sin \frac{\alpha}{2}, \quad (5)$$

where  $\lambda$  is the laser radiation wavelength. The main method to determine the frequency  $\omega_d$  is the spectral analysis of the photodetector signal. In the present paper the spectral analysis was implemented using the software, developed in the LabVIEW environment (National Instruments, USA). The photodetector signal was recorded using the ADC of the PC sound adapter with the frequency 44100 kHz and the resolution 16 bit. The spectrum estimate was found as the average over the non-overlapping modified periodograms with the Hanning data window [25].

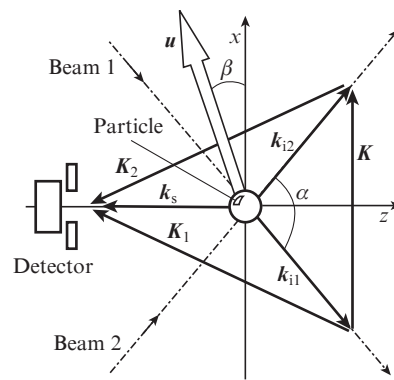


Figure 2. Scattering of laser radiation in the LDA probe volume.

When the concentration of scatterers in the flow is small, the LDA signal spectrum consists of two components [18, 19], one of them in the low-frequency region and the other in the high-frequency region

$$f_d = \frac{|\omega_d|}{2\pi} = \frac{1}{2\pi} |\mathbf{K}\mathbf{u}|. \quad (6)$$

The modulus means that the intensity variations at each point of the detector do not depend on the sign of  $\omega_d$  in the case when  $\delta$  is time-independent [see Eqn (3)]. Using Eqns (3) and (4) one can derive the expression for the magnitude of the particle velocity

$$u = \frac{\lambda_0}{2n \sin(\alpha/2) \cos \beta} f_d, \quad (7)$$

where  $\lambda_0$  is the radiation wavelength in free space;  $n$  is the refractive index of the medium, in which the angle between the beams is measured; and  $\beta$  is the angle between the directions of the particle velocity  $\mathbf{u}$  and the vector  $\mathbf{K}$  (Fig. 2). The proportionality coefficient between  $u$  and  $f_d$  remains constant under the translation of the probe volume through a planar boundary separating two media with different refractive indices if the boundary is perpendicular to the LDA optical axis. In this case the actual position of the probe volume is dis-

placed with respect to the crossing point of laser beam continuations in the first medium. The position of the probe volume with respect to the boundary between the media is determined by the relation [19]

$$\Delta z' \approx \Delta z(n'/n), \quad (8)$$

where  $\Delta z$  is the position of the crossing point of the laser beam continuations in the first medium with respect to the boundary separating the media; and  $n$  and  $n'$  are the refractive indices of the first and the second medium. It is also worth noting that in the scattering medium the contrast of the interference fringes is reduced due to the fluctuations of the laser radiation phase caused by the scattering.

#### 2.4. Scattering liquid flow

We used the channels with a rectangular-shaped cross section, formed by two microscope slides with the dimensions  $26 \times 76$  mm and the thickness 1.0 mm (AG00000102E, Menzel Glaser, Germany), between which the textolite or glass inserts of given thickness were placed (see Fig. 1). The obtained channels had the cross sections  $3 \times 6$ ,  $1 \times 2$  and  $0.25 \times 1$  mm (with the inserts having the thickness 3, 1 and 0.25 mm, respectively). Into the ends of the channels the metal tubes of the appropriate diameter were mounted, which were connected via flexible hoses with the inner diameter 3 mm with the system, providing the steady-state flow of the scattering liquid. The channels were installed in the holder equipped with the mechanism for micrometre displacement along the  $y$  and  $z$  axes (Fig. 1). The longitudinal axis of the channel was directed along the  $x$  axis. In order to protect the LDA objective from laser radiation specularly reflected from the channel window surface, the channel was slightly turned around the longitudinal axis so that the window plane made an angle of  $4^\circ$  with the  $y$  axis.

As a scattering liquid the suspension of kaolin particles in water and the rat blood were used. The mean size of kaolin particles was 1  $\mu\text{m}$ . The size was determined from the suspension images, obtained using the squashed drop method in transmitted light with the Axio Imager A1 microscope (Carl Zeiss, Germany) with the objective  $100\times$ , 0.7. In the experiments we used the solutions with the extinction coefficient up to  $2.7 \text{ mm}^{-1}$ . To ensure the suspension flow the channel was connected via flexible tubes with two cylindrical vessels with the diameter 200 mm, installed with the level difference 700 mm. The precise control of the flow velocity was implemented with the help of a screw clamp on the return line hose. Using 0.5 L of suspension, the system provides the constant flow velocity during 10 min.

The blood sample with the volume about 2 mL was taken from the aorta of a rat subjected to anesthetization. The number of erythrocytes in the sample, determined using the Goryaev chamber, amounted to  $7.5 \times 10^6 \mu\text{L}^{-1}$ , which corresponds to the norm for a healthy animal [26, 27]. The blood was let through the channel with the cross section  $0.25 \times 1$  mm by means of the 20-mL syringe, installed in the device for dosed injection of medical preparations.

The extinction coefficient  $\mu_t$  of the solutions was determined by measuring the collimated transmission with the setup, consisting of a semiconductor laser unit (FTI-Optronik, Russia) (the wavelength 650 nm, the power 5 mW, the beam divergence 6 mrad), a cuvette holder, two diaphragms with circular apertures 6 mm in diameter and a Laser Power Meter

815C (Newport, USA). The setup components were placed at the following distances from the laser module: the cuvette holder – 90 mm, the first diaphragm – 190 mm, the second diaphragm – 360 mm and the power meter sensor – 460 mm. To measure the collimated transmission of the solution two sequential measurements were performed: one with the cuvette filled with pure water, and the other with the cuvette filled with the solution under study. To measure the extinction coefficients  $\mu_1 < 0.5 \text{ mm}^{-1}$  we used the cuvette with the thickness 1 mm, and for optically denser suspensions the cuvette thickness was taken to be 340  $\mu\text{m}$ . The extinction coefficient of the whole blood determined by means of this setup amounted to  $11 \text{ mm}^{-1}$ .

### 3. Results and discussion

#### 3.1. Profile of the flow velocity distribution in a rectangular-shaped channel

To test the LDA operability we used a rectangular channel with a cross section  $3 \times 6$  mm. The suspension with the extinction coefficient  $0.3 \text{ mm}^{-1}$  was let through the channel. Figure 3a shows the fluctuation spectrum of the photodetector signal power, corresponding to the localisation of the probe volume at the axis of the flow in the channel. The power spectrum estimate was found as the average over 20 periodograms with the data window of 2048 samples. The maximum of the high-frequency component of the spectrum corresponds to the frequency  $f_d$ . Figure 3b shows the profile of the flow velocity distribution in the channel in the middle of its height. The profile was obtained by displacing the channel with respect to the LDA with the step 100  $\mu\text{m}$ . The actual position of the probe volume was calculated using Eqn (8). The points in Fig. 3b show the measurement results. The profile of the laminar flow velocity distribution at the channel half-height is close to parabolic [28]. The solid curve (3) shows the second-order polynomial regression, obtained using the least-square method. The regression curve was calculated using the points that correspond to the localisation of the probe volume inside the channel (black squares in Fig. 3b).

#### 3.2. LDA signal structure for the flow velocity measurement in a strongly scattering liquid

For studying the LDA signal structure in the case of measuring the flow velocity in strongly scattering suspensions we used the channel with the cross section  $1 \times 2$  mm. The LDA probe volume was located at the flow axis in the channel at the distance 0.5 mm from its front window. The spectra were obtained from the signal record during 10 s as an average over 861 periodograms with the window of 512 points. Figure 4a [curve (1)] shows the spectrum obtained for the suspension extinction coefficient  $\mu_1 = 1.5 \text{ mm}^{-1}$ . As  $\mu_1$  grows, the high-frequency component of the power spectrum, corresponding to the modulation of the scattered radiation, becomes smaller against the background of the low-frequency component.

The presence of a maximum at the frequency  $f_d$  in the LDA signal spectrum is caused by radiation of the first and the second beams, scattered by the particles that move in the overlap region, interfering at the detector. However, when the concentration of scatterers is high, radiation, scattered by the particles located in other parts of the flow and irradiated by only one of the probing laser beams, also arrives at the detec-

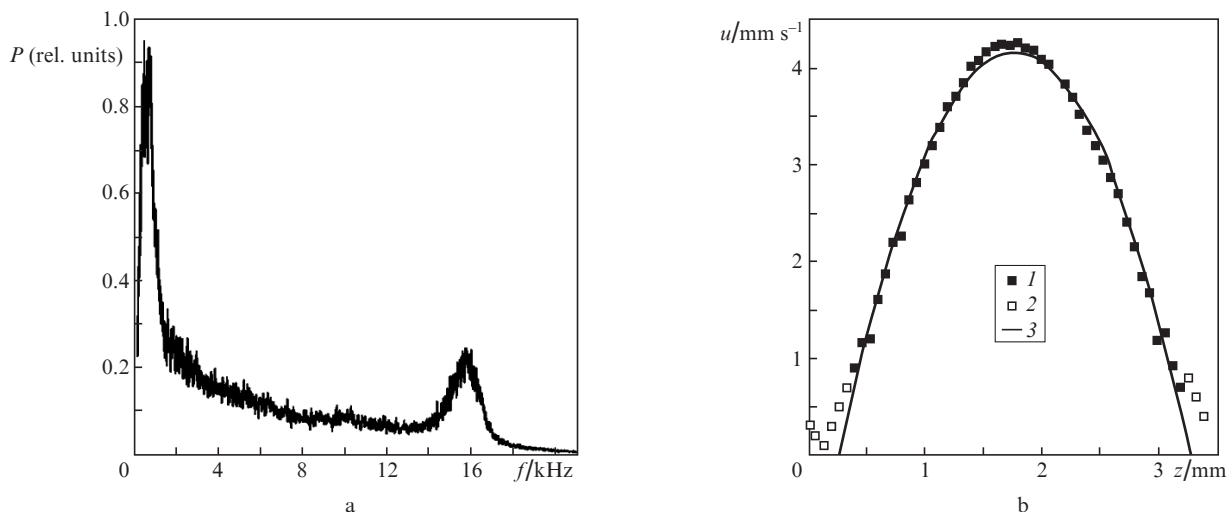


**Figure 3.** Power spectrum of the photodetector signal (a) and velocity distribution profile (b) of the flow  $u$  in the channel with a rectangular-shaped cross section  $3 \times 6$  mm; (1, 2) experimental data; (3) second-order polynomial regression line, calculated using the data of curve (1).

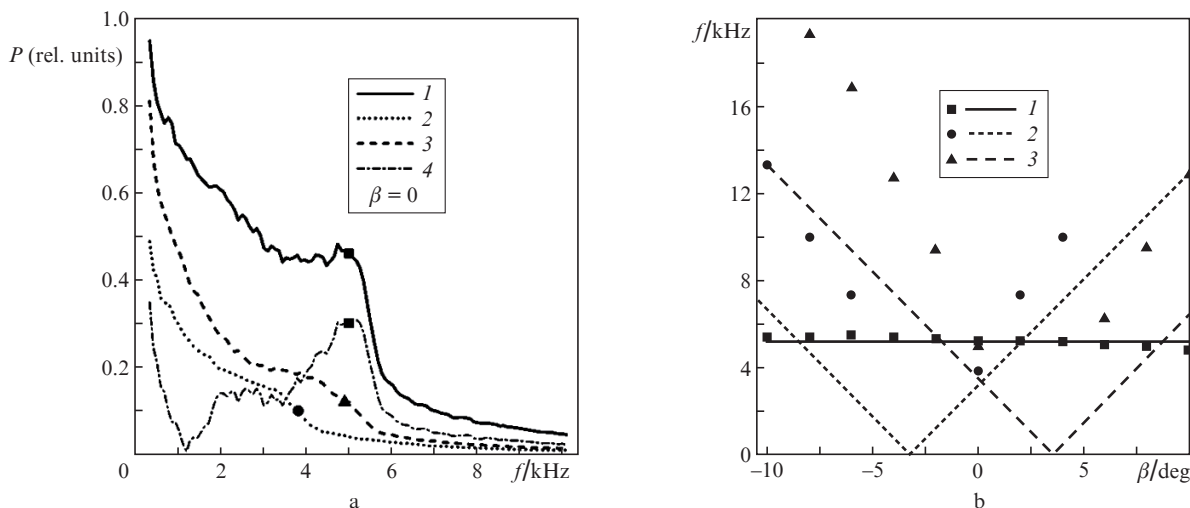


**Figure 4.** Power spectra of the LDA signal  $P_{12}(f)$  (1),  $P_1(f)$  (2),  $P_2(f)$  (3) and  $|P'_{12}(f)|$  (4); the points are the values of  $f_d$  (1, 4),  $f_1$  (2) and  $f_2$  (3) (a), and the dependence of the frequencies  $f_d$  (1),  $f_1$  (2) and  $f_2$  (3) on the angle  $\beta$ ; points show measured values, lines – calculated ones (b).

tor. The frequency of radiation scattered by an individual particle is given by Eqns (1) and (2). At different points of the channel the particles move with different velocities. As a result of the interference of the waves, scattered by different particles, in the LDA signal spectrum the components appear with the frequencies distributed within the interval from zero to a certain maximal frequency (referred to as a cutoff frequency) [4]. The cutoff frequency equals the difference between the frequencies of radiation scattered by the particle with the minimal possible velocity (i.e., not moving at all) and the particle with the maximal possible velocity at the flow axis. These components can be observed in the case when the channel is illuminated by only one of the two beams. Figure 4a shows the spectrum  $P_{12}(f)$  [curve (1)] of the signal, obtained under the illumination of the flow by two beams, and the spectra  $P_1(f)$  [curve (2)] and  $P_2(f)$  [curve (3)], obtained under the illumination of the channel by the left and the right beam separately (beam 1 and beam 3 in Fig. 2).

The spectra  $P_1(f)$  and  $P_2(f)$  apparently form the low-frequency pedestal that hides the peak at the frequency  $f_d$  in the spectrum  $P_{12}(f)$ . Neglecting the interference of the fields scattered by different particles, one can select the frequency components that correspond to the light scattered by the particles simultaneously illuminated by two beams (4) (Fig. 4a):

$$P'_{12}(f) = P_{12}(f) - P_1(f) - P_2(f). \tag{9}$$

The spectrum  $P'_{12}(f)$  has a pronounced maximum at the frequency  $f_d$ , coinciding with the maximum of  $P_{12}(f)$  (Fig. 4a). The differential spectrum has a pronounced maximum, corresponding to the frequency  $f_d$ . Thus, the calculation of  $P'_{12}(f)$  allows one to determine the frequency  $f_d$  in the measurement of the flow velocity in strongly scattering liquid even in the case when the expressed maximum in the LDA signal power spectrum is absent.

The spectra  $P_1(f)$  and  $P_2(f)$  were obtained with a single beam illuminating the flow in the channel (like in the LDA

schemes used in ophthalmology [1–5]). To measure the flow velocity in such a scheme, use is made of the value of the cutoff frequency in the spectrum of the photodetector signal, determined by fitting to the spectrum of the model, specified by the rectangular function [4]. The cutoff frequency in the case of using beams 1 and 2 can approximately correspond to the maximal possible Doppler frequency shift [see Eqns (1) and (2)]:

$$f_1 = \frac{|\omega_0 - \omega_1|}{2\pi} = \frac{1}{2\pi} |\mathbf{K}_1 \mathbf{u}|, f_2 = \frac{|\omega_0 - \omega_2|}{2\pi} = \frac{1}{2\pi} |\mathbf{K}_2 \mathbf{u}|, \quad (10)$$

where  $\mathbf{K}_1$  and  $\mathbf{K}_2$  are the vectors of scattering of beams 1 and 2 by the moving particles (see Fig. 2). The frequencies  $f_d$ ,  $f_1$ , and  $f_2$  depend on the angle between the optical axis of the device and the flow velocity vector. To study this dependence the channel with the cross section  $1 \times 2$  mm was installed on a rotary table that can rotate in the horizontal plane. The zero for the table rotation angle  $\beta$  was taken to correspond to the direction for which the channel axis is perpendicular to the LDA optical axis; and the flow velocity vector  $\mathbf{u}$  is parallel to the differential wave vector  $\mathbf{K}$  [see Fig. 2 and Eqn (7)]. The region of the LDA laser beam overlap was located at the suspension flow axis, the suspension extinction coefficient being equal to  $1.5 \text{ mm}^{-1}$ . For every position of the rotary table the LDA signal was recorded with the illumination by two beams and by each of the beams separately. The spectra, shown in Fig. 4a, correspond to  $\beta = 0$ . The frequency  $f_d$  was determined as the position of the maximum in the spectrum  $P_{12}(f)$  [points at curves (1) and (4) in Fig. 4a]. The frequencies  $f_1$  and  $f_2$  were determined at the half of the step height in the spectra  $P_1(f)$  and  $P_2(f)$  [points at curves (2) and (3) in Fig. 4a, respectively].

The dependence  $f_d(\beta)$  is shown in Fig. 4b. The points indicate the measured values, and the solid line corresponds to the dependence, calculated using Eqn (7) at a constant flow velocity  $1.4 \text{ mm s}^{-1}$ . The displacement of the experimental points with respect to the calculated line can be explained by the mismatch between the channel axis position and the table rotation axis, as well as by the displacement of the laser beams overlap region due to the refraction at the surfaces of the channel window [lines and points (2) and (3)]. Similarly, Fig. 4b presents the dependence of the frequencies  $f_1$  and  $f_2$  on the angle  $\beta$ . The points show the measured values, and the dashed lines correspond to the dependences, calculated using Eqns (10) at  $u = 1.4 \text{ mm s}^{-1}$ .

The scattering vectors  $\mathbf{K}_1$  and  $\mathbf{K}_2$  make the angles close to  $90^\circ$  with the flow velocity vector; therefore,  $f_1$  and  $f_2$  strongly depend on  $\beta$  and turn into zero if the velocity vector is perpendicular to the corresponding scattering vector. The measured values of the cutoff frequency are significantly higher than the calculated ones. This can be explained by the fact that Eqns (10) give the maximal possible frequency of the Doppler shift, while the cutoff frequency corresponds to the high-frequency boundary of the spectrum that can be shifted towards the short-wave region as a result of the spectrum broadening, associated with the light scattering in the flow and with the use of a wide-aperture detector.

### 3.3. Blood flow velocity measurement

Figure 5 shows the spectra  $P_{12}(f)$  obtained in the flow velocity measurements at the axis of the rectangular channel with the thickness  $250 \mu\text{m}$ , through which the blood diluted with saline

or the whole blood was flowing. The spectra were calculated using the records made during 2 s; the data window was 512 points. The maximum corresponding to the frequency  $f_d$  in these spectra can be recognised only when the blood is diluted by 50 times. For weaker dilution no pronounced maxima in the spectra can be observed. The amplitude of the LDA signal decreases with increasing extinction coefficient; therefore, for better comparison the spectra in Fig. 5 are normalised to the total power in the frequency band  $0.4\text{--}20$  kHz. Figure 5a shows the power spectra  $P_{12}(f)$  [curves (1)] and the corresponding positive values  $P'_{12}(f)$  [curves (2)]. The largest values of  $P'_{12}(f)$  are concentrated near the frequency  $f_d$ , corresponding to the mean motion velocity of the blood cells through the LDA probe volume. The maxima of  $P'_{12}(f)$  have a significant width, because the length of the LDA probe volume in this experiment is comparable with the channel thickness.

It is seen that the growth of the extinction coefficient does not virtually affect the maxima broadening. The results corresponding to the flow of the whole blood are presented in Fig. 6. In spite of the high extinction coefficient of blood and the significant channel thickness, the values of  $P'_{12}(f)$  [curve (3)] near  $f_d$  amount to almost 20% of the corresponding values of  $P_{12}(f)$  [curve (1)]. The dependence  $P'_{12}(f)$  (2), analogous to (4) in Fig. 4a, allows the estimation of the negative values of  $P'_{12}(f)$  in the low-frequency region. In the same Figure the dependence of the positive values  $P'_{12}(f)$  magnified by ten times is presented that demonstrates the high signal-to-noise ratio in the measurements of the whole blood flow velocity.

The obtained results demonstrate the possibility of using the differential LDA for *in vivo* measurements of the blood flow velocity in vessels with a diameter up to  $250 \mu\text{m}$ . For this goal the simplest version of the LDA can be applied that implies no preliminary relative frequency shift of the laser beams, which is used to determine the sign of  $f_d$  and to separate the high-frequency and low-frequency components in the LDA signal spectrum [19, 23, 24]. We have shown that the maximal contribution to the low-frequency component of the LDA spectrum in the case of measuring the flow velocity in a strongly scattering liquid is caused by the scattering of laser beams beyond the probe volume. These components can be eliminated from the signal spectrum by subtracting the spectra, obtained under separate illumination of the probe volume with each of the beams. The most important advantage of the differential LDA over the existing LDAs intended for ophthalmology [1–4] and the DOCT systems [6–9] is the weak dependence of the LDA signal on the angle between the axis of the optical system and the direction of the flow velocity in the most common case, when this angle is close to  $90^\circ$ .

The factors of primary importance that determine the precision of the blood flow velocity measurement are the selection of radiation, for which the direction of propagation before and after scattering by a moving particle is unchanged, and the spatial localisation of the volume, in which the scattering occurs. In the ophthalmologic LDAs, where the probe volume is illuminated with a single laser beam, such a selection is implemented by means of a confocal field stop, optically conjugated with the probe volume [5]. The field stop also provides the localisation of the probe volume in the lateral direction, but since the numerical aperture of the objective in such a system is small, the probe volume has significant extent along the optical axis, which leads to the characteristic step-wise shape of the spectrum [1–5]. The small detector aperture

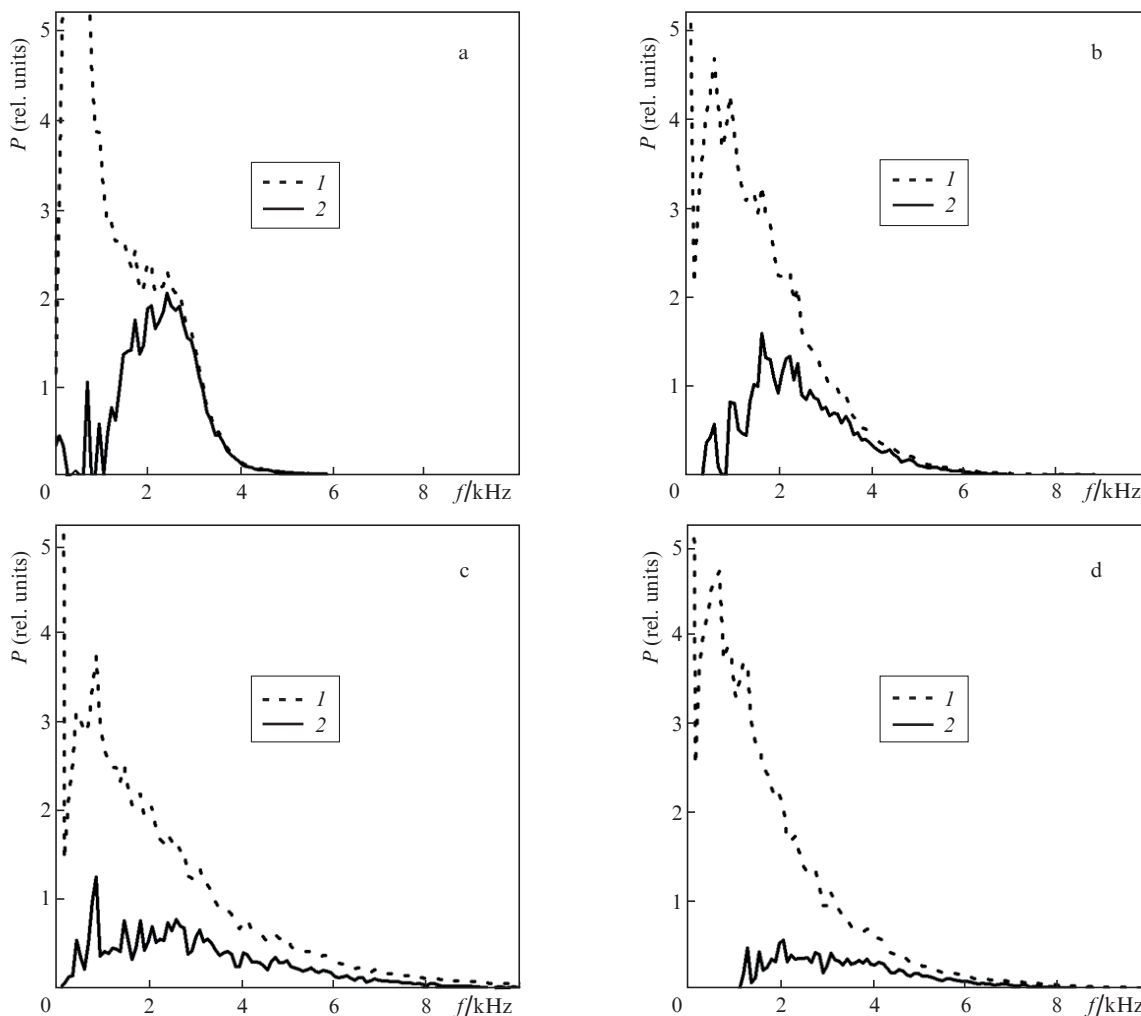


**Figure 5.** Normalised spectra  $P_{12}(f)$  (1) and positive values  $P'_{12}(f)$  (2) obtained by measuring the flow velocity of blood, diluted as 1:50 (a), 1:10 (b), 1:3 (c) and the whole blood (d) in the 250  $\mu\text{m}$  thick channel.

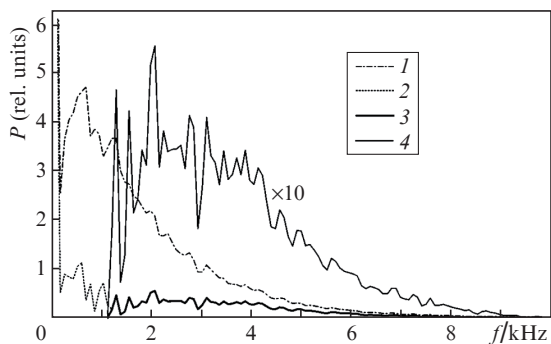


**Figure 6.** Spectra  $P_{12}(f)$  (1),  $|P'_{12}(f)|$  (2), positive values of  $P'_{12}(f)$  (3) and  $P'_{12}(f) \times 10$  (4) in the case of whole blood flow at the axis of the 250  $\mu\text{m}$  thick channel.

in the ophthalmologic LDAs is caused by the necessity of unambiguous determination of the wave vector  $k_s$  of the scattered light (see Fig. 2), rather than by the small aperture ratio of the eye. The ambiguity of this vector direction in the case of using a detector with a large numerical aperture leads to the step smoothing and hampers the cutoff frequency measurement. For example, in Fig. 5a the spectra  $P_1(f)$  and  $P_2(f)$  recorded using the detector with a numerical aperture 0.1 are

shown. In the DOCT systems [6–9] the longitudinal localisation of the probe volume is provided due to the interference selection of low-coherence radiation, scattered from a definite depth. Due to this the DOCT signal spectrum has an expressed maximum that corresponds to the DFS of the light, scattered at a definite point of the blood vessel.

In the differential LDA the longitudinal localisation of the probe volume is determined by the size of the laser beam overlap region. Although in our LDA the overlap region of the laser beams has the length of nearly 100  $\mu\text{m}$ , the major contribution to the LDA signal is produced by the particles that cross the probe volume in its median, largest cross section, conjugated with the detector field stop, i.e., the particles, crossing the beam just at the place of the largest cross section, stay illuminated by both beams together during the longest time.

### 4. Conclusions

We propose a new method for analysing the LDA signal based of the differential scheme, providing a high signal-to-noise ratio in the measurement of the flow velocity in strongly scattering liquids, such as whole blood in animal and human arterioles and venules. The possibility of measuring the flow velocity of whole blood in the channel with the thickness 250  $\mu\text{m}$  was demonstrated.

It is shown that when a blood vessel is probed in the direction, perpendicular to its axis, the result of the velocity measurement is practically independent of the angle between the LDA optical axis and the axis of the vessel within the angle variation range  $\pm 10^\circ$ . Thus, in contrast to the existing ophthalmologic [1–4] and DOCT systems [8, 9], the LDA proposed by us provides high-precision flow velocity measurement using a single DFS registration channel.

**Acknowledgements.** The work was performed within the State Task in the Field of Research Activity Programme No. 2014/203 NIR No. 1490 ‘Development of Optical Methods and Means of Controlling the Structure and Dynamics of Biological Media’.

## References

- Garhofer G., Werkmeister R., Dragostinoff N., Schmetterer L. *Inv. Ophth. Vis. Sci.*, **53** (2), 698 (2012).
- Cherecheanu P., Garhofer G., Schmidl D., Werkmeister R., Schmetterer L. *Curr. Opin. Pharmacol.*, **13**, 36 (2013).
- Pemp B., Polska E., Garhofer G., Bayerle-Eder M., Kautzky-Willer A., Schmetterer L. *Diabetes Care*, **33**, 2038 (2010).
- Riva C.E., in *Ocular Blood Flow* (Berlin, Heidelberg: Springer-Verlag, 2012).
- Logean E., Schmetterer L., Riva C.E. *Laser Phys.*, **13** (1), 45 (2003).
- Huang Y., Ibrahim Z., Tong D., Zhu S., Mao Q., Pang J., Lee W.P.A., Brandacher G., Kang J.U. *J. Biomed. Opt.*, **18** (11), 111404 (2013).
- Mahmud M.S., Cadotte D.W., Vuong B., Sun C., Luk T.W.H., Mariampillai A., Yang V.X.D. *J. Biomed. Opt.*, **18** (5), 050901 (2013).
- Trasischker W., Werkmeister R.M., Zotter S., Baumann B., Torzicky T., Pircher M., Hitzenberger C.K. *J. Biomed. Opt.*, **18** (11), 116010 (2013).
- Doblhoff-Dier V., Schmetterer L., Vilser W., Garhofer G., Gröschl M., Rainer A.L., Werkmeister R.M. *Biomed. Opt. Express*, **5** (2), 630 (2014).
- Egawa G., Nakamizo S., Natsuaki Y., et al. *Sci. Rep.*, **3**, 1932 (2013).
- Vieira de Moraes L., Tadokoro C.E., et al. *PLOS Pathogens*, **9** (1), e1003154 (2013).
- Pinhas A., Dubow M., Shah N., Chui T.Y., Scoles D., Sulai Y.N., Weitz R., Walsh J.B., Carroll J., Dubra A., Rosen R.B. *Biomed. Opt. Express*, **4** (8), 1305 (2013).
- Jia Y., Morrison J.C., Tokayer J., Tan O., Lombardi L., Baumann B., Lu C.D., Choi W.J., Fujimoto J.G., Huang D. *Biomed. Opt. Express*, **3** (12), 3127 (2012).
- Leahy M.J. (Ed.) *Microcirculation Imaging* (Blackwell: Wiley, 2012) p. 411.
- Briers D., Duncan D.D., Hirst E.R., et al. *J. Biomed. Opt.*, **18** (6), 066018 (2013).
- Feuerstein D., Takagaki M., Gramer M., Manning A., Endepols H., Vollmar S., Yoshimine T., Strong A.J., Graf R., Backes H. *J. Cerebral Blood Flow Metabolism*, **53**, 10.1038 (2014).
- Silvestre J.S., Smadja D.M., Lévy B.I. *Physiol. Rev.*, **93** (4), 1743 (2013).
- Fedosov I.V., Tuchin V.V., in: *Coherent-Domain Optical Methods: Biomedical Diagnostics, Environmental Monitoring and Material Science*. Ed. by V.V. Tuchin (Berlin, Heidelberg, NY: Springer-Verlag, 2013) p. 487–564.
- Zhang Z. *LDA Application Methods* (Berlin, Heidelberg: Springer-Verlag, 2010) p. 274.
- Pedersen C.J., Huang D., Shure M.A., Rollins A.M. *Opt. Lett.*, **32** (5), 506 (2007).
- Wang Y., Bower B.A., Izatt J.A., Tan O., Huang D. *J. Biomed. Opt.*, **13** (6), 064003 (2008).
- Srinivasan V.J., Sakadžić S., Gorczynska I., Ruvinskaya S., Wu W., Fujimoto J.G., Boas D.A. *Opt. Express*, **18** (3), 2477 (2010).
- Levenko B.A., Priezhev A.V., Proskurin S.G., Savchenko N.B. *Izv. Ross. Akad. Nauk, Ser. Fiz.*, **59** (6) (1995).
- Nagai M., Matsuda K., Ohtsubo J., Homma K., Shimizu K. *Opt. Eng.*, **32** (1), 15 (1993).
- Welch P.D. *IEEE Trans. Audio Electro Acoustics*, **AU-15** (2), 70 (1967).
- Bernardi C., Moneta D., Brughera M., Di Salvo M., Lamparelli D., Mazu G., Iatropoulos M.J. *Comp. Haematol. Int.*, **6**, 160 (1996).
- Tuchin V.V. (Ed.) *Handbook of Optical Biomedical Diagnostics* (Bellingham: SPIE Press, 2002).
- Pozrikidis C. *Fluid Dynamics: Theory, Computation, and Numerical Simulation* (Springer Science + Business Media, LLC, 2009) p.763.